Structural and biochemical analyses of the nuclear IκBζ protein in complex with the NF-κB p50 homodimer

Norman Zhu,[1] W. Eric Rogers,[1] David K. Heidary,[2] and Tom Huxford[1]

[1]Structural Biochemistry Laboratory, Department of Chemistry and Biochemistry, San Diego State University, San Diego, California 92182, USA; [2]Department of Chemistry, North Carolina State University, Raleigh, North Carolina 27607, USA

As part of the efforts to understand nuclear IκB function in NF-κB-dependent gene expression, we report an X-ray crystal structure of the IκBζ ankyrin repeat domain in complex with the dimerization domain of the NF-κB p50 homodimer. IκBζ possesses an N-terminal α helix that conveys domain folding stability. Affinity and specificity of the complex depend on a small portion of p50 at the nuclear localization signal. The model suggests that only one p50 subunit supports binding with IκBζ, and biochemical experiments confirm that IκBζ associates with DNA-bound NF-κB p50:RelA heterodimers. Comparisons of IκBζ:p50 and p50:κB DNA complex crystallographic models indicate that structural rearrangement is necessary for ternary complex formation of IκBζ and p50 with DNA.

Supplemental material is available for this article.

Received May 4, 2024; revised version accepted June 13, 2024.

Regulation of transcription factor NF-κB occurs primarily through its noncovalent association with ankyrin repeat-containing inhibitor proteins of the IκB family (Hinz et al. 2012). In resting cells, IκBα sequesters NF-κB dimers to the cytoplasm by masking the nuclear localization signal (NLS) of individual NF-κB subunits and contributing its own potential for export from the nucleus (Malek et al. 1998; Johnson et al. 1999; Huang et al. 2000). Diverse cellular stress signals trigger induction of NF-κB transcriptional activity through a highly regulated mechanism involving site-specific phosphorylation and ubiquitin-dependent 26S proteasome-mediated degradation of IκBα (Karin and Ben-Neriah 2000; Hayden and Ghosh 2008). This results in the rapid nuclear accumulation of NF-κB, whereupon it binds with DNA sequence specificity to promoter and enhancer elements, leading to the expression of response genes. The entire process takes place within a matter of minutes and requires no new protein synthesis (Hoffmann et al. 2002).

Among the NF-κB-dependent gene products that result from extracellular signaling by interleukin-1 (IL-1) or bacterial lipopolysaccharide (LPS) is the protein IκBζ (Kitamura et al. 2000; Haruta et al. 2001; Yamazaki et al. 2001). Newly translated IκBζ localizes to the nucleus when overexpressed in cells and coimmunoprecipitates preferentially with the NF-κB p50 subunit. Generation and characterization of IκBζ-null mice revealed that, although viable, mice without IκBζ suffer from atopic dermatitis (Shiina et al. 2004; Yamamoto et al. 2004). Peritoneal macrophages derived from these animals are incapable of producing the pluripotent cytokine interleukin-6 (IL-6) in response to stimulation by LPS. IL-6 is a known NF-κB-dependent gene that promotes cell growth and has been implicated in numerous inflammatory diseases as well as cancer (Libermann and Baltimore 1990; Shimizu et al. 1990; Karin 2006). However, its expression in wild-type mouse peritoneal macrophage cells lags that of early NF-κB-dependent genes, with mRNA not observed until >2 h after induction with LPS (Yamamoto et al. 2004). Therefore, it appears that IκBζ, an early gene product of NF-κB-dependent transcription, participates directly through the NF-κB p50 subunit in the nucleus to commence late expression of additional NF-κB-dependent genes such as IL-6 (Smale 2010; Tartey et al. 2014).

In order to gain greater insight into the affinity and specificity-determining elements of NF-κB:IκB complexes in general and to shed light on the molecular mechanism of IκBζ function in cells, we have determined a 2.0 Å X-ray cocrystal structure of the C-terminal ankyrin repeat domain of human IκBζ in complex with the dimerization domain of the NF-κB p50 homodimer. This work represents the first X-ray structure of a nuclear IκB protein in complex with NF-κB and the first complex of the NF-κB p50 homodimer with another protein. The model and accompanying in vitro biochemical studies revealed that IκBζ possesses a unique N-terminal α helix that conveys folding stability to the ankyrin repeat domain and that complex affinity and specificity are driven by a relatively small portion of p50 that includes the NLS. Interestingly, the crystallographic model suggests that only one p50 subunit is required to support complex formation with IκBζ, and binding experiments confirm that IκBζ interacts with κB DNA-bound NF-κB p50:RelA heterodimers. Finally, comparison of the IκBζ:p50 complex structural model and the X-ray crystal structure of the p50 homodimer in complex with κB DNA from the promoter of the human IL-6 gene indicates that structural rearrangements are necessary to support ternary complex formation of IκBζ and p50 with DNA.

Results and Discussion

X-ray crystal structure of an IκBζ:NF-κB p50 homodimer complex

Working with purified recombinant proteins, we previously demonstrated that the nuclear IκB protein IκBζ binds with high affinity to NF-κB p50 subunit homodimers and not to NF-κB RelA homodimers (Trinh et al. 2008). This is

[*Keywords*: IκBζ; NF-κB; protein structure; transcription regulation; X-ray crystallography]
Corresponding author: thuxford@sdsu.edu
Article published online ahead of print. Article and publication date are online at http://www.genesdev.org/cgi/doi/10.1101/gad.351892.124.

in direct contrast to the classical cytoplasmic IκBα protein that binds stably to RelA but not to p50 homodimers. In an effort to identify a chemical basis for this binding selectivity, we crystallized and determined the X-ray cocrystal structure of the human IκBζ C-terminal ankyrin repeat domain (residues 404–718) with a murine p50 dimerization domain homodimer (residues 245–376) (Fig. 1A; Supplemental Figs. S1, S2). Attempts at crystallization of a ternary IκBζ:p50 homodimer:κB DNA complex were unsuccessful, as IκBζ proteins formed a precipitate in the presence of κB DNA at concentrations typically required for protein complex cocrystallization.

The IκBζ:p50 complex cocrystal structure was solved by molecular replacement and refined against complete diffraction data to a resolution of 2.0 Å, resulting in a high-quality model with excellent stereochemistry (Supplemental Table S1). The crystallographic model reveals that IκBζ interacts with the p50 homodimer in a manner analogous to how IκBα contacts p50:RelA heterodimers or how IκBβ interacts with homodimers of RelA (Fig. 1B; Huxford et al. 1998; Jacobs and Harrison 1998; Malek et al. 2003). IκBζ contacts both p50 subunits along the dimer interface, roughly orthogonal to the homodimer C2 symmetry axis, resulting in unique interactions with different faces of each of the two p50 subunits (model chains B and C). Of the solvent-exposed surface area, 4030 $Å^2$ is buried upon complex formation, which is comparable with similar complexes of NF-κB dimers with IκBα and IκBβ. Of this binding interface, 2900 $Å^2$ derives from IκBζ contacting p50 chain B, which occupies the same position as the critical RelA subunit within the IκBα:p50:RelA complex.

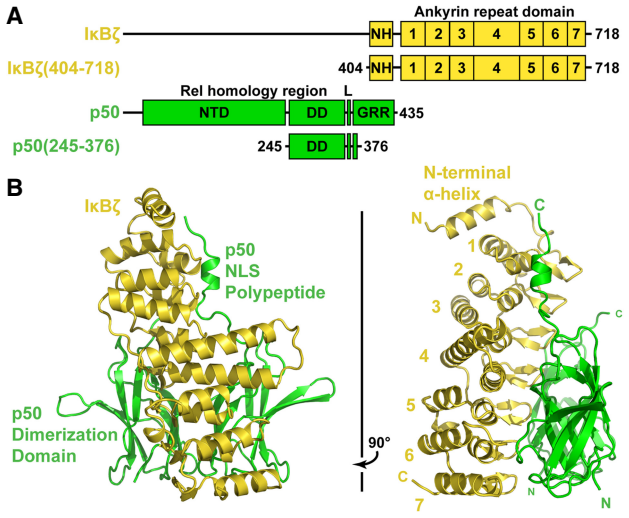

Figure 1. X-ray crystal structure of a human IκBζ:NF-κB p50 homodimer complex. (*A*) Domain organization schematics of full-length (*top*) and crystallized (*bottom*) protein constructs of IκBζ (yellow) and the NF-κB p50 subunit (green). The position of the N-terminal α helix (NH) is labeled, and individual ankyrin repeats are numbered (1–7) on IκBζ. The N-terminal domain (NTD), dimerization domain (DD), NLS polypeptide (L), and glycine-rich region (GRR) of p50 are labeled. Amino acid numbering reflects the human IκBζ long isoform and the murine p50 subunit. (*B*, *left* panel) Ribbon diagram representation of IκBζ (yellow) in complex with p50 (green), viewed perpendicular to the twofold axis of the p50 homodimer. The lone ordered p50 NLS polypeptide from p50 subunit chain B is labeled. (*Right* panel) The same model rotated 90° about the *y*-axis. The N and C termini of the individual polypeptides are indicated (N and C, respectively), the N-terminal α helix of IκBζ is labeled, and each ankyrin repeat is numbered (1–7).

IκBζ ankyrin repeat domain structure and stability

IκBζ exhibits the characteristic ankyrin repeat domain fold, with seven clear ankyrin repeats. The nuclear IκB protein Bcl-3 as well as the C-terminal portion of the p100 NF-κB precursor protein, itself also a bona fide IκB, also contain seven ankyrin repeats, while both IκBα and IκBβ have six (Michel et al. 2001; Basak et al. 2007; Tao et al. 2014). IκBζ is unique among all IκB proteins in that the IκBζ amino acid sequence ends abruptly with its seventh ankyrin repeat, in contrast to the other family members that possess functionally and/or structurally relevant elements C-terminal to their ankyrin repeat domains (Supplemental Fig. S1). In the crystallographic model, we did not observe electron density for the extreme C-terminal residues 710–718, suggesting that they adopt multiple conformations throughout the crystal.

Ankyrin repeat 4 consists of 61 amino acids, 28 amino acids more than the consensus, resulting in the extension of both α helices of ankyrin repeat 4 by roughly three turns. This creates a protuberance that contributes additional contacts with p50 chain B. Intriguingly, IκBζ residue Glu569 from the extended inner α helix of ankyrin repeat 4 is positioned within close proximity to p50 Lys315, an amino acid residue that is unique to p50 among the otherwise highly conserved NF-κB subunits (Supplemental Figs. S1, S2).

Another striking structural difference in IκBζ relative to other IκB proteins is the presence of an N-terminal α helix (residues 417–429) above ankyrin repeat 1. Superposition of the IκBζ:p50 crystallographic model with a similar subcomplex from the IκBα:p50:RelA crystal structure reveals that this IκBζ N-terminal α helix contributes nonpolar amino acid side chains that bury against ankyrin repeat 1 in a manner similar to residues from the RelA subunit atop IκBα (Fig. 2A). Biochemical studies of IκBα:RelA binding revealed the importance of these N-terminal nonpolar capping interactions in conferring folding stability to IκBα and contributing significantly to IκBα:RelA complex binding affinity (Cervantes et al. 2011). In order to test whether the IκBζ N-terminal α helix plays a similar stabilizing role in IκBζ, we engineered a construct consisting of IκBζ residues 437–718 that lacks the N-terminal structural element. Treatment of GST-IκBζ(404–718) with trace amounts of chymotrypsin revealed that a substantial amount of the protein remained intact even after 2 h, while similar treatment of GST-IκBζ(437–718) renders it susceptible to rapid proteolysis, leaving behind only the GST protein (Fig. 2B). Further investigation into thermal denaturation of the two IκBζ proteins by circular dichroism (CD) spectroscopy revealed that IκBζ(404–718) displays a clear folded-to-unfolded transition at 40.7°C, while IκBζ(437–718) exhibits solution behavior that is consistent with an unfolded state across the entire range of temperatures measured (Fig. 2C). Chemical denaturation with urea followed by CD spectroscopy revealed similar trends (Supplemental Fig. S3). Intriguingly, we observed via pull-down experiments that GST-IκBζ(404–718), but not GST-IκBζ(437–718), associates with p50 homodimers in vitro (Supplemental Fig. S4). This experiment also established that the p50 homodimer does not interact nonspecifically with free GST protein or glutathione

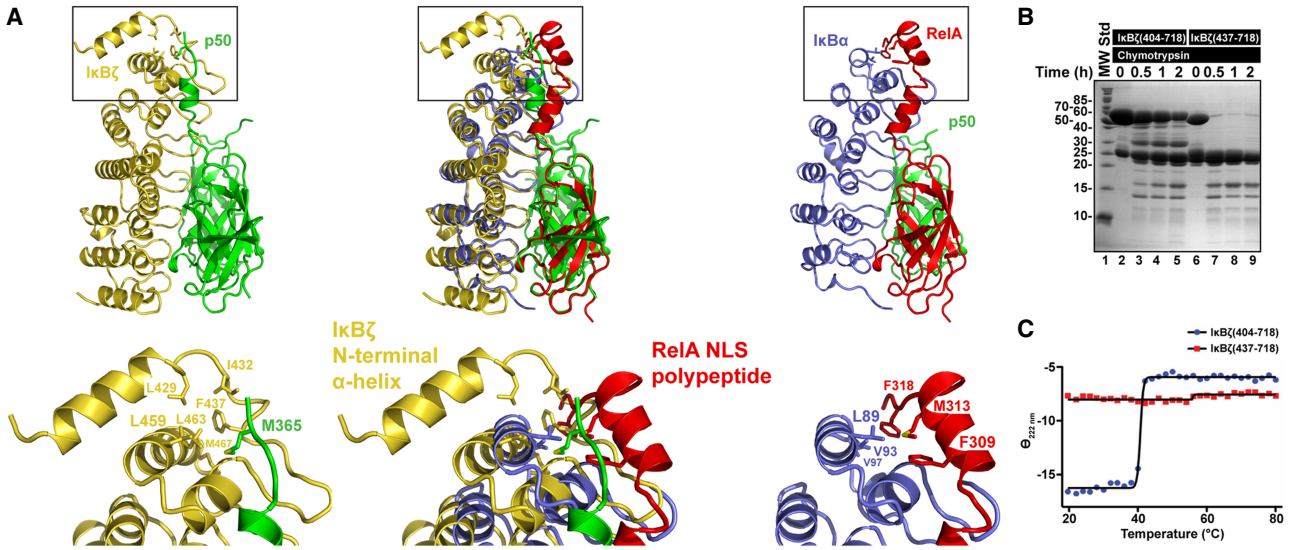

Figure 2. An N-terminal α helix stabilizes the IκBζ ARD. (*A*) The IκBζ:p50 (*top left*) and IκBα:p50:RelA (*top right*) complexes are viewed similarly as ribbon diagrams. In the *middle*, the two complexes are superposed with respect to the dimerization domains. Close-up views of the boxed regions illustrate the nonpolar interactions that cap ankyrin repeat 1 of the IκBζ:p50 (*bottom left*) and IκBα:p50:RelA (*bottom right*) complexes. In both complexes, nonpolar amino acids from the outer α helix of ankyrin repeat 1 are buried. However, in IκBζ, the majority of nonpolar amino acids that cap ankyrin repeat 1 derive from the N-terminal α helix, whereas IκBα relies on nonpolar residues from the NLS polypeptide of the RelA subunit. The overlay reveals similarities in the positions of nonpolar capping residues in the two complexes. (*B*) Coomassie-stained SDS-PAGE shows the GST-IκBζ(404–718) protein is resistant to proteolysis with limiting amounts of chymotrypsin even after 2 h (lanes *2–5*), while similar amounts of GST-IκBζ(404–718), which lacks the N-terminal α helix, are rapidly degraded (lanes *6–9*). (*C*) Circular dichroism (CD) measurement of ellipticity at 222 nm during thermal denaturation reveals a clear loss of folded structure by IκBζ(404–718) at 40.7°C, while IκBζ(437–718) behaves as a disordered protein across the entire range of temperatures tested.

Sepharose beads. Therefore, it appears that the N-terminal α helix conveys overall folding stability to the IκBζ ankyrin repeat domain in a manner analogous to that observed by the RelA NLS polypeptide and IκBα and that this stability contributes to NF-κB p50 homodimer binding.

Residues within the p50 subunit NLS polypeptide dictate IκBζ binding specificity

The most strikingly unique interactions within the complex involve direct hydrogen bonding between residues from ankyrin repeats 1–3 of IκBζ and the p50 chain B NLS polypeptide. Several residues from both proteins drive structural stabilization of the otherwise disordered p50 NLS, including Glu477, His478, and Arg514 from IκBζ and Lys354, Glu355, and Glu356 in p50 (Fig. 3A; Supplemental Figs. S1, S2). Additional hydrogen bond contacts between IκBζ residues Asp411 and Asp443 and p50 NLS residues Lys360 and Lys363 are conserved in other IκB:NF-κB complexes, previously having been implicated in the interaction between p50 and the nuclear IκB protein Bcl-3 (Collins et al. 2015). Based on the unique sequence and structure of these interacting elements, we hypothesized that they form the basis for high affinity and selective binding of IκBζ to the NF-κB p50 subunit.

To test this, we exploited the fact that IκBζ binds to homodimers of p50 but not the structurally homologous RelA and measured the effect of swapping the NLS-containing polypeptides from one protein to the other. Previously, we reported that transfer of murine RelA subunit amino acids 291–333 (containing the entire NLS polypeptide region) to the corresponding region on p50 was necessary but not sufficient to render the resulting chimeric fusion protein a high-affinity binding partner for IκBα. Conversion of p50 to a protein that binds IκBα with affinity nearly equivalent to that of RelA required the additional transfer of Asn202 and Ser203 from within the dimerization domain of RelA to p50 (Huxford et al. 2002). For the present study, we performed GST pull-downs with purified native and chimeric NF-κB p50 and RelA homodimers and GST-IκBζ(404–718) and determined that transfer of p50 subunit amino acids 350–376 (containing the entire p50 NLS polypeptide) was sufficient to convert RelA into a high-affinity binding partner with IκBζ (Fig. 3B).

In order to provide a more quantitative assessment of binding affinity, surface plasmon resonance (SPR) spectroscopy was used to determine on-rate and off-rate kinetic constants for IκBζ toward different NF-κB p50 and RelA homodimers (Fig. 3C). Binding affinity (K_D) for IκBζ(404–718) and p50(245–376) by this method was measured at 91.2 pM, which is on par with what we have previously reported for IκBζ:p50 complexes (Trinh et al. 2008). Removal of the p50 NLS polypeptide resulted in a p50(245–350) homodimer for which no binding to IκBζ(404–718) could be detected by SPR. Similarly, the affinity of IκBζ(404–718) for the RelA(191–325) homodimer, which displays subnanomolar binding affinity for IκBα and IκBβ, was below the limit of detection by SPR. Replacement with the p50 NLS polypeptide, however, converted RelA into a RelA(191–290)–p50(350–376) chimeric fusion protein that bound to IκBζ(404–718) with a K_D of 615 pM (Supplemental Fig. S5). Thus, we conclude that residues within the p50 NLS polypeptide are necessary for the observed high-affinity binding of IκBζ to p50 and that this element is sufficient for conferring high-affinity IκBζ binding to RelA. Finally, it bears mentioning that the NF-κB p52

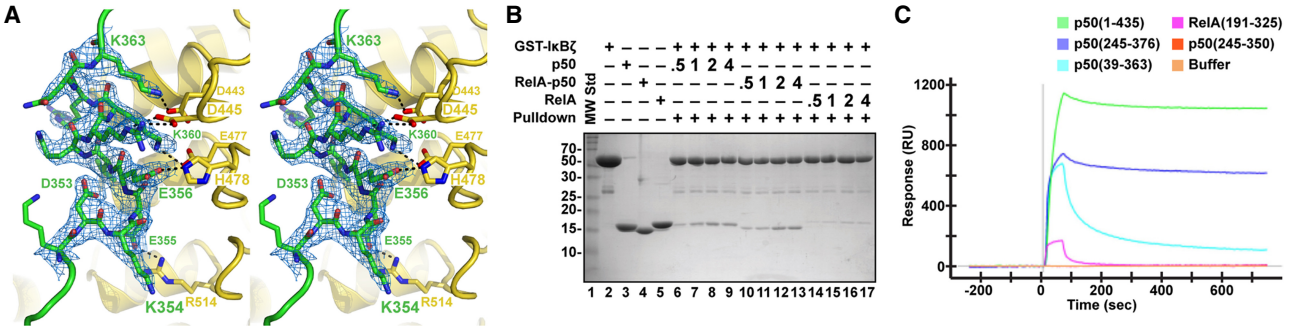

Figure 3. The p50 NLS polypeptide dictates IκBζ binding affinity and specificity. (*A*) A stereo view of the refined $2F_O$-F_C electron density map contoured at 1.1 σ (blue mesh) about the NF-κB p50 subunit chain B NLS polypeptide (represented as green sticks) and bound to ankyrin repeats 1–3 of IκBζ (depicted in yellow). The electron density in this region is representative of the quality throughout the entire map. Several key residues are numbered, and intermolecular hydrogen bonds between charged amino acid side chains are depicted as black dashed lines. (*B*) Coomassie-stained SDS-PAGE analysis of GST pull-downs with purified recombinant proteins reveals that transfer of the p50 NLS polypeptide (residues 350–376) to the dimerization domain of RelA results in a RelA(191–290)–p50(350–376) chimeric fusion protein that interacts with GST-IκBζ (404–718) to an extent similar to p50(245–376) (cf. lanes *6–9* and *10–13*). RelA(191–325), in contrast, does not show increased binding above background to GST-IκBζ. A GST/glutathione Sepharose bead control is shown in Supplemental Figure S4. (*C*) Surface plasmon resonance (SPR) sensorgrams show that an intact NLS polypeptide in p50(1–435) or p50(245–376) insures high-affinity binding to IκBζ(404–718). Partial disruption makes p50(39–363) a poorer binder, and complete removal renders p50(245–350) incapable of binding at all. Binding by RelA(191–325) also falls outside the range of measurement.

subunit contains residues identical to p50 Lys354, Glu355, and Glu356 as well as Lys360 and Lys363 at equivalent positions, and that Glu477 and His478 from IκBζ are also present in the nuclear IκB protein IκBNS (Supplemental Figs. S1, S2).

IκBζ interacts similarly with p50 homodimers and p50:RelA heterodimers on κB DNA

The observation that IκBζ contacts only one of two p50 subunit NLS polypeptides in the otherwise symmetrical p50 homodimer raised the possibility that it might also be capable of similar p50 subunit binding with the ubiquitous NF-κB p50:RelA heterodimer. Superposition of the p50:RelA heterodimer from the IκBα:p50:RelA complex crystal structure onto IκBζ:p50 suggests that the RelA subunit could occupy the position of p50 chain C in IκBζ:p50 without disrupting the structure of IκBζ or the p50 dimer interface (Supplemental Fig. S6A). It also suggests that simultaneous binding of IκBα and IκBζ to p50:RelA heterodimers would not be possible, as the two bound inhibitor proteins would force collisions with one another (Supplemental Fig. S6B).

To further test the hypothesis that IκBζ requires only one p50 subunit for binding to NF-κB dimers, we performed electrophoretic mobility supershift assays by adding GST-IκBζ(404–718) to purified recombinant NF-κB p50 homodimers, p50:RelA heterodimers, and RelA homodimers in complex with a radiolabeled κB DNA probe from the promoter of the human IL-6 gene. We previously demonstrated that IκBα removed RelA from IL-6 κB DNA and did not interact with the p50:IL-6 κB DNA complex, while IκBζ failed to remove RelA from IL-6 κB DNA and caused the p50:IL-6 κB DNA complex to shift to a higher molecular weight, consistent with a ternary IκBζ:p50:DNA complex (Trinh et al. 2008). In the present study, we report that the addition of IκBζ(404–718) to preformed p50:RelA:IL-6 κB DNA complexes resulted in the appearance of a supershifted band that is qualitatively identical to that observed upon incubation with p50:IL-6 κB DNA complexes but not with RelA:IL-6 κB DNA (Fig. 4A). This strongly suggests that IκBζ possesses a similar propensity for interaction and ternary complex formation with p50 homodimers and p50:RelA heterodimers on κB DNA.

A recently published genome-wide analysis of nascent transcription in Toll-like receptor 4 (TLR4)-activated macrophages reported that, in addition to association with the majority of p50 subunit-dependent genes, IκBζ displays considerable overlap with RelA and that many p50:IκBζ-dependent genes contain sites at which association with both RelA and IκBζ was dependent on p50 (Daly et al. 2024). These findings suggest that, through its association with p50, IκBζ contributes to RelA-dependent gene expression, significantly expanding the potential of IκBζ as a transcriptional coregulator for the vast collection of NF-κB-dependent genes.

Ternary IκBζ:p50:DNA complex formation requires structural rearrangement

Superposition of the NF-κB p50 dimerization domains from the IκBζ:p50 complex model onto the same dimerization domains in the recently published p50:IL-6 κB DNA complex crystal structure reveals practically no change in their structures. However, even cursory inspection suggests that, without some structural rearrangement, ankyrin repeat 7 of IκBζ clashes severely with κB DNA (Fig. 4B). It is possible that the extreme C-terminal residues 410–418 of IκBζ, which were disordered in the crystal, might play some role in mediating this structural rearrangement upon binding to κB DNA. IκBζ could then use its extensive N-terminal portions to mediate interactions with chromatin remodeling and transcriptional coactivators, as has been proposed (Tartey et al. 2014). Asymmetric binding of NF-κB subunits on DNA has been observed previously, and recent structural evidence that the dimerization domains of the p50 homodimer are capable of moving relative to DNA to accommodate different spacing at target κB DNA binding sites suggests that IκBζ could facilitate such protein structural rearrangements in a manner that supports stable ternary complex formation

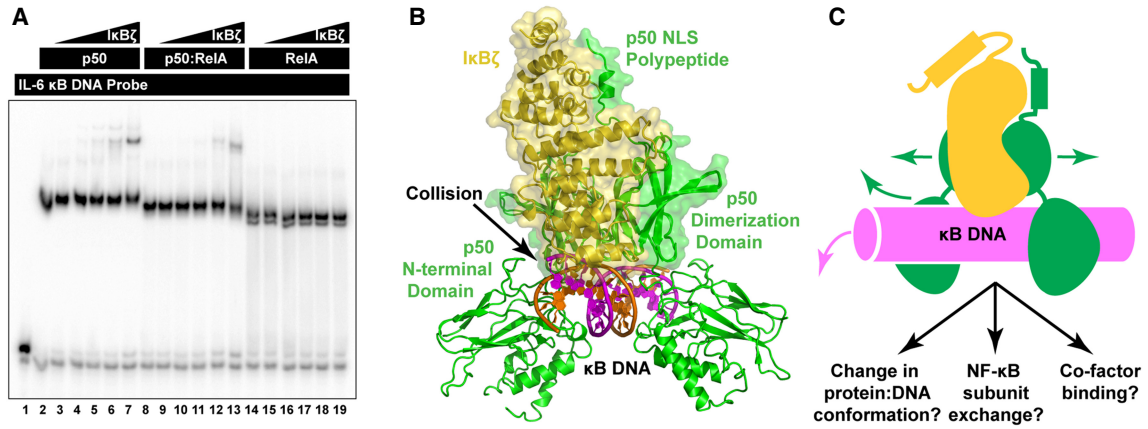

Figure 4. IκBζ interacts similarly with NF-κB p50 homodimers and p50:RelA heterodimers on κB DNA. (*A*) Native polyacrylamide gel electrophoretic mobility shift assay of the recombinant purified p50(1–376) homodimer (lanes *2–7*), p50(1–376):RelA(1–325) heterodimer (lanes *8–13*), and RelA(1–325) homodimer (lanes *14–19*) in the presence of increasing concentrations of GST-IκBζ(404–718) reveals similar supershifting of p50 and p50:RelA (cf. lanes *7* and *13*) but not RelA (lane *19*). (*B*) Composite model created by superposition of the dimerization domains from the IκBζ:p50 complex crystal structure and the crystallographic model of the p50:IL-6 κB DNA complex (PDB ID: 8TKM) illustrates that ternary IκBζ:p50:DNA complex formation would result in collision of IκBζ (yellow) and DNA (magenta:orange). (*C*) A schematic representation of the IκBζ ankyrin repeat domain (yellow) interacting with the NF-κB p50 homodimer (green) on DNA (magenta). Structural rearrangement of DNA and/or p50 domains is required to accommodate IκBζ binding.

(Chen et al. 1998; Zhu et al. 2023). It is also possible, particularly in light of the observations that it can mediate interactions with NF-κB p50:RelA heterodimers on κB DNA, that IκBζ binding might serve to destabilize one NF-κB p50 homodimer subunit relative to the other in a manner that facilitates its replacement with other transcription factors such as RelA (Fig. 4C). Further biochemical and transcription-based studies will be required to unravel the precise structural consequences of IκBζ association with NF-κB homodimers or heterodimers on κB DNA in the nucleus.

Materials and methods

DNA plasmids

A plasmid containing the full-length human IκBζ cDNA was graciously provided by T. Muta. DNA fragments encoding amino acids 404–718 or 437–718 were amplified by PCR with primers containing restriction sites and ligated into the BamHI and NotI sites of the pHIS8 and pGEX4T-2 vectors. Murine p50 deletion and p50–RelA fusion chimeric protein expression plasmids were described previously (Huxford et al. 2002; Trinh et al. 2008).

Protein expression and purification

His-tagged IκBζ(404–718) and IκBζ(437–718) plasmids were transformed into chemically competent BL21(DE3) *Escherichia coli* and cultured in 2 L of LB with 25 μg/mL kanamycin sulfate. Cells were isolated by centrifugation at 4000*g* for 10 min, resuspended in lysis buffer (25 mM Tris-HCl at pH 7.4, 500 mM NaCl, 0.5 mM EDTA, 10 mM β-mercaptoethanol, 10 mM imidazole), and lysed by two passages through a M110L microfluidizer (Microfluidics). Lysates were clarified by centrifugation at 12,000*g*, passed through a 0.8 μm filter followed by affinity purification at 4°C on a Ni Sepharose Fast Flow (GE Healthcare) column, and eluted in lysis buffer with 250 mM imidazole. Affinity purification of glutathione-S-transferase (GST) and GST-IκBζ proteins was carried out with a glutathione Sepharose 4 Fast Flow column (GE Healthcare). Purification of untagged recombinant murine NF-κB p50 protein constructs in addition to chimeric NF-κB proteins was carried out by ion exchange chromatography using SP Sepharose Fast Flow resin (GE Healthcare). All proteins were then further purified by size exclusion chromatography and stored at –80°C, as described previously (Huxford et al. 2002; Trinh et al. 2008).

IκBζ:p50 complex formation and cocrystallization

To avoid aggregation, Ni affinity-purified IκBζ(404–718) protein was immediately combined at a 1:4 molar ratio with excess size exclusion-purified p50(245–376), and the mixture was dialyzed with three changes against 1 L of 25 mM Tris-HCl (pH 7.4), 500 mM NaCl, 0.5 mM EDTA, and 10 mM β-mercaptoethanol to remove imidazole. Recombinant thrombin (Sigma) was added at a ratio of 1 U per 100 μg of His-tagged IκBζ(404–718) and incubated overnight at 4°C with gentle stirring before halting the reaction by addition of 0.5 mM phenylmethylsulfonylfluoride followed by size exclusion purification on a Superdex 200 26/60 column. Peak fractions were analyzed by SDS-PAGE and concentrated by a Centriprep 30 (Millipore) to 13 mg/mL, flash-cooled in 26 μL aliquots, and stored at –80°C. IκBζ(404–718):p50(245–718) complex cocrystals were grown by hanging drop vapor diffusion in which 1 μL of protein complex was mixed with 1 μL of reservoir solution (20 mM acetic acid at pH 5.2, 80 mM acetic acid at pH 5.8, 5.5% [w/v] PEG 3350, 10 mM DTT, 0.5% 1,2,3-heptanetriol) and sealed over 1 mL of reservoir solution. Needle clusters containing some rod-like crystals grew in 2–3 days at 30°C.

X-ray diffraction data collection

IκBζ:p50 homodimer complex cocrystals were harvested with nylon loops and flash-cooled in 20 mM Na acetate (pH 5.2), 80 mM Na acetate (pH 5.8), 16% (w/v) PEG 3350, 10 mM DTT, 0.5% 1,2,3-heptanetriol, and 22% (v/v) 2-methyl-2,4-pentanediol. Synchrotron X-ray diffraction data were collected at 100 K on an ADSC Q315 CCD detector at the Advanced Light Source Beamline 8.2.2, Lawrence Berkeley National Laboratory. Data processing was carried out in HKL2000 (Otwinowski and Minor 1997). Data collection statistics are presented in Supplemental Table S1.

Structure solution and refinement

Multibody molecular replacement was performed in PHASER using as probes the p50 dimerization domain (PDB ID: 1BFS) and the ankyrin repeat domain of Bcl-3 (PDB ID: 1K1A) with ions, ligands, and solvent molecules removed (Huang et al. 1997; Michel et al. 2001). Rigid body maximum likelihood refinement was run in RefMac5 (Murshudov et al. 1997). The resulting model was built into difference electron density maps in COOT before further cycles of refinement in PHENIX (Adams et al. 2010; Emsley et al. 2010). Stereochemical analysis and final adjustments to the model were directed by MolProbity (Chen et al. 2010). Atomic coordinates for the IκBζ:p50 complex crystal structure have been submitted to the Protein Data Bank and assigned PDB ID 9BOR. Surface area calculations and figures were prepared in PyMol (DeLano 2002). Model refinement statistics are presented in Supplemental Table S1.

Limited proteolysis digestion

Purified recombinant GST-IκBζ(404–718) and GST-IκBζ (437–718) (100 µL of each) were combined at 1.6 mg/mL concentration with 0.05 U/µL chymotrypsin (CalBiochem) in 25 mM Tris-HCl (pH 7.5), 50 mM NaCl, and 1 mM DTT and incubated in a 37°C water bath. During the assay, 15 µL (24 µg of GST-IκBζ) of reaction samples was removed at the 0, 30, 60, and 120 min time points; halted by the addition of 5 µL of 4× Laemmli buffer; and then heated for 5 min to 98°C. Digested products were stored on ice, analyzed by 12.5% SDS-PAGE, and stained with Coomassie.

Circular dichroism spectroscopy

CD measurements were carried out on a J-815 spectropolarimeter equipped with a Peltier temperature control unit (Jasco). Thermal denaturation experiments were performed on both IκBζ(404–718) and IκBζ(437–718) at 0.18 mg/mL in 50 mM K_2HPO_4 (pH 7.6) and 10 mM NaCl. The temperature was raised from 20°C to 80°C, and ellipticity at 222 nm was measured every 2°C, while full spectra from 190–250 nm were collected every 10°C. For chemical denaturation experiments, similar samples were prepared at urea concentrations of 0, 0.5, 1, 2, 4, and 8 M and allowed to incubate for 1 h at room temperature. Full spectra were collected on IκBζ(404–718) at all urea concentrations, while full spectra on IκBζ(437–718) were collected at 0 and 7.5 M urea concentrations only. Ellipticity at 222 nm was recorded for both proteins at all urea concentrations.

Site-directed mutagenesis

Engineering, expression, and purification of chimeric p50 (245–349)–RelA(290–333) and RelA(191–290)–p50(350–376) proteins by cation exchange and size exclusion chromatography were described previously (Huxford et al. 2002).

GST pull-downs

Reactions (250 µL) were prepared with 1 mg/mL GST-IκBζ (404–718) and 0.1–4 µM NF-κB proteins in 25 mM Tris-HCl (pH 7.4), 40 mM NaCl, and 1 mM DTT. Twenty microliters of glutathione Sepharose 4 Fast Flow beads suspended in the same buffer was added to each reaction and allowed to incubate with gentle rotation for 10 min at room temperature. Beads were pelleted at 7000*g* for 1 min. The supernatant was removed without disturbing the resin, washed three times in 1 mL of buffer, and rotated for 5 min. The supernatant was removed and beads were resuspended in 20 µL of 2× Laemmli buffer, heated for 5 min at 98°C, and analyzed on a 12.5% SDS-PAGE stained by Coomassie.

Surface plasmon resonance spectroscopy

Sensorgrams were recorded on a Bio-Rad Proteon XPR36 instrument using a His tag capture chip (Bio-Rad) as previously described (Trinh et al. 2008). Briefly, 5 µg/mL His-tagged IκBζ(404–718) in 10 mM Na phosphate (pH 7.4), 150 mM NaCl, 0.05% Tween-20, and 0.05% BSA was passed over and allowed to bind to the chip. Recombinant native sequence and mutated and chimeric p50 proteins at five different concentrations ranging from 3.12 to 50 nM were then passed simultaneously over the chip at 100 µL/min, and the rates of binding and dissociation were monitored for 150 sec. Sensorgrams were analyzed under a homogenous single-state binding model by ProteOn Manager version 2.0 software (Bio-Rad). All experiments were performed at 25°C.

Electrophoretic mobility shift assay

Electrophoretic mobility shift analysis of a radiolabeled κB DNA probe and purified NF-κB and IκB proteins has been described previously (Trinh et al. 2008). Briefly, a PAGE-purified human IL-6 κB oligonucleotide of sequence 5′-AGATTTATCAAATGTGGGATTTTCCCATGAGTC TCAATATT-3′ (IDT oligos; κB DNA is underlined) was radiolabeled with ^{32}P-γ-ATP (Perkin Elmer) using T4 polynucleotide kinase (New England Biolabs) prior to annealing with its complementary sequence oligo. Purified recombinant NF-κB p50 homodimer, p50:RelA heterodimer, or

RelA homodimer proteins were combined with increasing amounts of GST-IκBζ(437–718) and incubated for 30 min in 10 mM Tris-HCl (pH 7.5), 50 mM NaCl, 10% (v/v) glycerol, 1% (v/v) NP-40, 1 mM EDTA, 0.1 mg/mL poly(dI-dC), 0.2 mg/mL BSA, and 1 mM DTT prior to addition of 0.002 μCi of IL-6 κB DNA probe. Native polyacrylamide gel electrophoresis was performed with continuous recirculating of 1× TGE buffer (24.8 mM Tris base, 190 mM glycine, 1 mM EDTA at pH 8.0). Reactions were run in triplicate, and the order of mixing did not affect results.

Competing interest statement

The authors declare no competing interests.

Acknowledgments

We thank T. Muta for human IκBζ cDNA, C. Ralston for synchrotron X-ray data collection support, M. Zhu at Bio-Rad for support with surface plasmon resonance spectroscopy, and S. Yamazaki and S.T. Smale for helpful discussions and encouragement. The Berkeley Center for Structural Biology is supported in part by the National Institutes of Health, the National Institute of General Medical Sciences, and the Howard Hughes Medical Institute. The Advanced Light Source is supported by the Director, Office of Science, Office of Basic Energy Sciences, of the U.S. Department of Energy under contract number DE-AC02-05CH11231. N.Z. and W.E.R. were both recipients of the Arne N. Wick Predoctoral Fellowship, and biochemistry research at San Diego State University is supported in part by the California Metabolic Research Foundation.

Author contributions: N.Z. conceived the study, performed the investigation and formal analysis, visualized the data, and wrote the original draft of the manuscript. W.E.R. performed the formal analysis and visualized the data. D.K.H. performed the investigation and the formal analysis. T.H. conceived the study, performed the investigation and formal analysis, acquired the funding, wrote the original draft of the manuscript, and reviewed and edited the manuscript.

References

Adams PD, Afonine PV, Bunkóczi G, Chen VB, Davis IW, Echols N, Headd JJ, Hung LW, Kapral GJ, Grosse-Kunstleve RW, et al. 2010. PHENIX: a comprehensive Python-based system for macromolecular structure solution. *Acta Crystallogr D Biol Crystallogr* **66:** 213–221. doi:10.1107/S0907444909052925

Basak S, Kim H, Kearns JD, Tergaonkar V, O'Dea E, Werner SL, Benedict CA, Ware CF, Ghosh G, Verma IM, et al. 2007. A fourth IκB protein within the NF-κB signaling module. *Cell* **128:** 369–381. doi:10.1016/j.cell.2006.12.033

Cervantes CF, Bergqvist S, Kjaergaard M, Kroon G, Sue SC, Dyson HJ, Komives EA. 2011. The RelA nuclear localization signal folds upon binding to IκBα. *J Mol Biol* **405:** 754–764. doi:10.1016/j.jmb.2010.10.055

Chen YQ, Ghosh S, Ghosh G. 1998. A novel DNA recognition mode by the NF-κB p65 homodimer. *Nat Struct Biol* **5:** 67–73. doi:10.1038/nsb0198-67

Chen VB, Arendall WB III, Headd JJ, Keedy DA, Immormino RM, Kapral GJ, Murray LW, Richardson JS, Richardson DC. 2010. MolProbity: all-atom structure validation for macromolecular crystallography. *Acta Crystallogr D Biol Crystallogr* **66:** 12–21. doi:10.1107/S0907444909042073

Collins PE, Grassia G, Colleran A, Kiely PA, Ialenti A, Maffia P, Carmody RJ. 2015. Mapping the interaction of B cell leukemia 3 (BCL-3) and nuclear factor κB (NF-κB) p50 identifies a BCL-3-mimetic anti-inflammatory peptide. *J Biol Chem* **290:** 15687–15696. doi:10.1074/jbc.M115.643700

Daly AE, Yeh G, Soltero S, Smale ST. 2024. Selective regulation of a defined subset of inflammatory and immunoregulatory genes by an NF-κB p50–IκBζ pathway. *Genes Dev* (this issue). doi:10.1101/gad.351630.124

DeLano WL. 2002. *The PyMOL molecular graphics system*. DeLano Scientific, Palo Alto, CA.

Emsley P, Lohkamp B, Scott WG, Cowtan K. 2010. Features and development of Coot. *Acta Crystallogr D Biol Crystallogr* **66:** 486–501. doi:10.1107/S0907444910007493

Haruta H, Kato A, Todokoro K. 2001. Isolation of a novel interleukin-1-inducible nuclear protein bearing ankyrin-repeat motifs. *J Biol Chem* **276:** 12485–12488. doi:10.1074/jbc.C100075200

Hayden MS, Ghosh S. 2008. Shared principles in NF-κB signaling. *Cell* **132:** 344–362. doi:10.1016/j.cell.2008.01.020

Hinz M, Arslan SC, Scheidereit C. 2012. It takes two to tango: IκBs, the multifunctional partners of NF-κB. *Immunol Rev* **246:** 59–76. doi:10.1111/j.1600-065X.2012.01102.x

Hoffmann A, Levchenko A, Scott ML, Baltimore D. 2002. The IκB–NF-κB signaling module: temporal control and selective gene activation. *Science* **298:** 1241–1245. doi:10.1126/science.1071914

Huang DB, Huxford T, Chen YQ, Ghosh G. 1997. The role of DNA in the mechanism of NF-κB dimer formation: crystal structures of the dimerization domains of the p50 and p65 subunits. *Structure* **5:** 1427–1436. doi:10.1016/S0969-2126(97)00293-1

Huang TT, Kudo N, Yoshida M, Miyamoto S. 2000. A nuclear export signal in the N-terminal regulatory domain of IκBα controls cytoplasmic localization of inactive NF-κB/IκBα complexes. *Proc Natl Acad Sci* **97:** 1014–1019. doi:10.1073/pnas.97.3.1014

Huxford T, Huang DB, Malek S, Ghosh G. 1998. The crystal structure of the IκBα/NF-κB complex reveals mechanisms of NF-κB inactivation. *Cell* **95:** 759–770. doi:10.1016/S0092-8674(00)81699-2

Huxford T, Mishler D, Phelps CB, Huang DB, Sengchanthalangsy LL, Reeves R, Hughes CA, Komives EA, Ghosh G. 2002. Solvent exposed non-contacting amino acids play a critical role in NF-κB/IκBα complex formation. *J Mol Biol* **324:** 587–597. doi:10.1016/S0022-2836(02)01149-X

Jacobs MD, Harrison SC. 1998. Structure of an IκBα/NF-κB complex. *Cell* **95:** 749–758. doi:10.1016/S0092-8674(00)81698-0

Johnson C, Van Antwerp D, Hope TJ. 1999. An N-terminal nuclear export signal is required for the nucleocytoplasmic shuttling of IκBα. *EMBO J* **18:** 6682–6693. doi:10.1093/emboj/18.23.6682

Karin M. 2006. Nuclear factor-κB in cancer development and progression. *Nature* **441:** 431–436. doi:10.1038/nature04870

Karin M, Ben-Neriah Y. 2000. Phosphorylation meets ubiquitination: the control of NF-κB activity. *Annu Rev Immunol* **18:** 621–663. doi:10.1146/annurev.immunol.18.1.621

Kitamura H, Kanehira K, Okita K, Morimatsu M, Saito M. 2000. MAIL, a novel nuclear IκB protein that potentiates LPS-induced IL-6 production. *FEBS Lett* **485:** 53–56. doi:10.1016/S0014-5793(00)02185-2

Libermann TA, Baltimore D. 1990. Activation of interleukin-6 gene expression through the NF-κB transcription factor. *Mol Cell Biol* **10:** 2327–2334. doi:10.1128/mcb.10.5.2327-2334.1990

Malek S, Huxford T, Ghosh G. 1998. IκBα functions through direct contacts with the nuclear localization signals and the DNA binding sequences of NF-κB. *J Biol Chem* **273:** 25427–25435. doi:10.1074/jbc.273.39.25427

Malek S, Huang DB, Huxford T, Ghosh S, Ghosh G. 2003. X-ray crystal structure of an IκBβ–NF-κB p65 homodimer complex. *J Biol Chem* **278:** 23094–23100. doi:10.1074/jbc.M301022200

Michel F, Soler-Lopez M, Petosa C, Cramer P, Siebenlist U, Müller CW. 2001. Crystal structure of the ankyrin repeat domain of Bcl-3: a unique member of the IκB protein family. *EMBO J* **20:** 6180–6190. doi:10.1093/emboj/20.22.6180

Murshudov GN, Vagin AA, Dodson EJ. 1997. Refinement of macromolecular structures by the maximum-likelihood method. *Acta Crystallogr D Biol Crystallogr* **53:** 240–255. doi:10.1107/S0907444996012255

Otwinowski Z, Minor W. 1997. Processing of X-ray diffraction data collected in oscillation mode. *Methods Enzymol* **276:** 307–326. doi:10.1016/S0076-6879(97)76066-X

Shiina T, Konno A, Oonuma T, Kitamura H, Imaoka K, Takeda N, Todokoro K, Morimatsu M. 2004. Targeted disruption of MAIL, a nuclear IκB protein, leads to severe atopic dermatitis-like disease. *J Biol Chem* **279:** 55493–55498. doi:10.1074/jbc.M409770200

Shimizu H, Mitomo K, Watanabe T, Okamoto S, Yamamoto K. 1990. Involvement of a NF-κB-like transcription factor in the activation of the interleukin-6 gene by inflammatory lymphokines. *Mol Cell Biol* **10:** 561–568. doi:10.1128/mcb.10.2.561-568.1990

Smale ST. 2010. Selective transcription in response to an inflammatory stimulus. *Cell* **140:** 833–844. doi:10.1016/j.cell.2010.01.037

Tao Z, Fusco A, Huang DB, Gupta K, Young Kim D, Ware CF, Van Duyne GD, Ghosh G. 2014. p100/IκBδ sequesters and inhibits NF-κB through κBsome formation. *Proc Natl Acad Sci* **111:** 15946–15951. doi:10.1073/pnas.1408552111

Tartey S, Matsushita K, Vandenbon A, Ori D, Imamura T, Mino T, Standley DM, Hoffmann JA, Reichhart JM, Akira S, et al. 2014. Akirin2 is critical for inducing inflammatory genes by bridging IκBζ and the SWI/SNF complex. *EMBO J* **33:** 2332–2348. doi:10.15252/embj.201488447

Trinh DV, Zhu N, Farhang G, Kim BJ, Huxford T. 2008. The nuclear IκB protein IκBζ specifically binds NF-κB p50 homodimers and forms a ternary complex on κB DNA. *J Mol Biol* **379:** 122–135. doi:10.1016/j.jmb.2008.03.060

Yamamoto M, Yamazaki S, Uematsu S, Sato S, Hemmi H, Hoshino K, Kaisho T, Kuwata H, Takeuchi O, Takeshige K, et al. 2004. Regulation of Toll/IL-1-receptor-mediated gene expression by the inducible nuclear protein IκBζ. *Nature* **430:** 218–222. doi:10.1038/nature02738

Yamazaki S, Muta T, Takeshige K. 2001. A novel IκB protein, IκBζ, induced by proinflammatory stimuli, negatively regulates nuclear factor-κB in the nuclei. *J Biol Chem* **276:** 27657–27662. doi:10.1074/jbc.M103426200

Zhu N, Mealka M, Mitchel S, Milani C, Acuña LM, Rogers E, Lahana AN, Huxford T. 2023. X-ray crystallographic study of preferred spacing by the NF-κB p50 homodimer on κB DNA. *Biomolecules* **13:** 1310. doi:10.3390/biom13091310